Earth-viewing satellite perspectives on the Chelyabinsk meteor event

Steven D. Miller[a,1], William C. Straka III[b], A. Scott Bachmeier[b], Timothy J. Schmit[c], Philip T. Partain[a], and Yoo-Jeong Noh[a]

[a]Cooperative Institute for Research in the Atmosphere, Colorado State University, Fort Collins, CO 80523; [b]Cooperative Institute for Meteorological Satellite Studies, University of Wisconsin–Madison, Madison, WI 53706; and [c]Advanced Satellite Products Branch, Center for Satellite Applications and Research, National Oceanic and Atmospheric Administration, Madison, WI 53715

Edited by Mark H. Thiemens, University of California, San Diego, La Jolla, CA, and approved September 19, 2013 (received for review April 29, 2013)

Large meteors (or superbolides [Ceplecha Z, et al. (1999) *Meteoroids 1998*:37–54]), although rare in recorded history, give sobering testimony to civilization's inherent vulnerability. A not-so-subtle reminder came on the morning of February 15, 2013, when a large meteoroid hurtled into the Earth's atmosphere, forming a superbolide near the city of Chelyabinsnk, Russia, ∼1,500 km east of Moscow, Russia [Ivanova MA, et al. (2013) *Abstracts of the 76th Annual Meeting of the Meteoritical Society*, 5366]. The object exploded in the stratosphere, and the ensuing shock wave blasted the city of Chelyabinsk, damaging structures and injuring hundreds. Details of trajectory are important for determining its specific source, the likelihood of future events, and potential mitigation measures. Earth-viewing environmental satellites can assist in these assessments. Here we examine satellite observations of the Chelyabinsk superbolide debris trail, collected within minutes of its entry. Estimates of trajectory are derived from differential views of the significantly parallax-displaced [e.g., Hasler AF (1981) *Bull Am Meteor Soc* 52:194–212] debris trail. The 282.7 ± 2.3° azimuth of trajectory, 18.5 ± 3.8° slope to the horizontal, and 17.7 ± 0.5 km/s velocity derived from these satellites agree well with parameters inferred from the wealth of surface-based photographs and amateur videos. More importantly, the results demonstrate the general ability of Earth-viewing satellites to provide valuable insight on trajectory reconstruction in the more likely scenario of sparse or nonexistent surface observations.

asteroids | atmospheric entry | remote sensing | multiangle | trajectory estimation

At ∼0320 UTC (∼9:20 AM, local time) on February 15, 2013, a large meteoroid entered Earth's atmosphere, tearing across the morning sky near Chelyabinsk, Russia (55.17°N, 61.40°E), an industrial city located near the southern Ural Mountains, ∼1,500 km southeast of Moscow (1). The previously uncatalogued meteoroid, with an estimated diameter of ∼15–20 m, mass of ∼7,000–10,000 tons, and a velocity of ∼18 km/s, formed a superbolide (2) and exploded in the stratosphere with an estimated total energy release of roughly 100–500 kilotons TNT (3).

Although we often think of Earth's atmosphere as being a tenuous media, an object entering it at speeds ranging from 12 to 20 km/s (or 50–60 times that of a typical bullet) experiences a strong mechanical shock. For noniron meteoroids <100 m in size, the most common result is catastrophic fragmentation and production of an airburst explosion high above the surface, with the level of maximum energy deposition at lower altitudes for more vertical trajectories and higher for more oblique ones (4). Such was the case with the Chelyabinsk superbolide, whose high-altitude explosion produced a powerful shock wave that blasted the city below, damaging structures and injuring hundreds. Only a scattering of fragments survived the entry and no impact crater was found, although shortly after the event the Chelyabinsk regional police department discovered a ∼6 m wide circular hole in an ice-covered lake near Chebarkul (54.96°N, 60.33°E), presumably formed by one of the larger meteorites. In this regard the Chelyabinsk events draws close parallels to the Tunguska event of June 30, 1908, when a stony meteoroid estimated to be of size ∼50 m left no hallmark crater but its shock wave caused widespread devastation over 2,200 km^2 of Siberian forest (5).

As it disintegrated in the atmosphere, the Chelyabinsk superbolide left a distinctive trail of dust, smoke, and ice debris. It can be readily inferred from numerous surface-based photographs and videos of this trail that the object approached the region from the east at a highly oblique (low elevation) angle, and disintegrated in the middle atmosphere. Using an array of georeferenced satellite imagery, which readily observed the debris trail shortly after formation, we attempted to quantify those notional observations and provide a top–down perspective on this rare event.

Available Satellite Observations

Several Earth-viewing environmental satellites in both geostationary and polar orbits (6) viewed the Chelyabinsk region within minutes of the superbolide, capturing the debris trail left as it passed through the middle atmosphere. The geostationary systems included several members of the European Organisation for the Exploitation of Meteorological Satellites (EUMETSAT) constellation (Meteosat-7, -8, -9, and -10); the Chinese Meteorological Administration Feng-Yun 2D; the Korean Meteorological Administration Communication, Ocean, Meteorological Satellite; and the Japanese Meteorological Administration Multifunctional Transport Satellite (MTSAT). These satellites, flying 35,786 km along the equatorial plane with orbital periods matching Earth's rotation rate (geostationary orbits), effectively hover

Significance

Satellite observations of large meteors (superbolides) offer important insight on trajectory through the atmosphere, and by extension, to orbital parameters that enable source attribution. On February 15, 2013, at 0920 local time, a superbolide exploded in the stratosphere near Chelyabinsk, Russia, issuing a large shock wave that damaged structures and injured hundreds below. The event was captured by Earth-viewing environmental satellites that provided multiangle views of the debris trail within minutes of formation. This paper documents these observations and their use to derive trajectory details. Results compare favorably with surface-based camera/video estimates, demonstrating the unconventional utility of satellites to characterize events that are more likely to occur away from a dense surface network.

Author contributions: S.D.M. designed research; S.D.M. and W.C.S. performed research; S.D.M., W.C.S., and A.S.B. contributed new reagents/analytic tools; S.D.M., W.C.S., A.S.B., T.J.S., P.T.P., and Y.-J.N. analyzed data; and S.D.M. wrote the paper.

The authors declare no conflict of interest.

This article is a PNAS Direct Submission.

Freely available online through the PNAS open access option.

Database deposition: Additional satellite information, including animations, can be found at cimss.ssec.wisc.edu/goes/blog/archives/12356.

[1]To whom correspondence should be addressed. E-mail: Steven.Miller@colostate.edu.

This article contains supporting information online at www.pnas.org/lookup/suppl/doi:10.1073/pnas.1307965110/-/DCSupplemental.

over a given location and provide 15–30-min imagery refresh rate. However, the high-latitude (~55°N) Chelyabinsk region resides near the limb of their views, compromising the spatial resolution quality of the imagery.

Complementing the geostationary observations was a serendipitously well-timed overpass from the polar-orbiting Defense Meteorological Satellite Program (DMSP) constellation F-16 satellite and its Operational Linescan System (OLS) sensor, which provided a unique west/northwestern perspective on the meteor trail. Considering the nature of the DMSP orbits (inclined ~98° to the equatorial plane, ~830 km altitude, and ~101-min orbital period), which offer global coverage but poor refresh at any given location, the space/time proximity of F-16 to the meteor's entry (0324:40 UTC, or within 5 min) was as fortunate as it was useful to the meteor trajectory calculations.

Conventional environmental satellites use scanning radiometers to image the Earth scene. Unlike a camera, which observes its entire field of regard during a single exposure period, scanning radiometers sample only a small instantaneous geometric field of view (e.g., a 1–4-km area of surface) at a time. The sensor scans (e.g., in a raster or pendulumlike motion) one line at a time to construct the full coverage of the domain. The sampling time interval defines the spatial resolution of each picture element (pixel) along the scan line. For example, a Meteosat-9 "full disk" high-resolution visible-band image contains 11,136 scan lines with 7,848 pixels per line. Any given pixel in the image is observed over a unique time interval lasting typically for less than a millisecond. The motion/evolution of meteorological features over these small time differences is considered negligible. However, the chances of such a scanning system capturing the actual object itself, which is moving across the scene at ~15–20 km/s, are vanishingly small. Instead, the satellite imagery captures the debris trail left in the wake of the object's traverse, and we can use details of the trail's location to infer trajectory of travel through the atmosphere.

The Earth-viewing satellites observed the Chelyabinsk meteor trail via assorted optical spectrum measurements, including standard bands centered in the visible (~0.6 μm), near-infrared window (~3.9 μm), water vapor (~6.7 μm), and thermal infrared window (~10.8 μm). The visible band measures reflected sunlight, the thermal infrared window measures thermal emission, and the near-infrared band is sensitive to both reflected solar and thermal emissions. For the purpose of estimating trajectory, the visible and thermal infrared window bands were used. Unfortunately, no space-borne active sensor observations [e.g., CloudSat radar, ref. 7; or Cloud-Aerosol Lidar and Infrared Pathfinder Satellite Observations (CALIPSO) lidar, ref. 8] were available for direct measurement of plume altitude or its internal structure properties, and the DMSP Nadir Photometer System sensor does not operate on the day side of the orbit (and even so, was too far west of the event to provide useful information).

Initial Observations

Within hours of the event, satellite images of the meteor debris trail began circulating through various media sources worldwide. The majority of examples came from various geostationary satellites mentioned above, and the Meteosat constellation members in particular. A compilation these geostationary observations are included in *Supporting Information* (Figs. S1–S5). Of particular interest among these were the Meteosat Second Generation (MSG) satellites; Meteosat-8 (located, on February 15, 2013, at 1.20°N, 4.24°E), Meteosat-9 (0.13°N, 9.46°E), and Meteosat-10 (1.06°S, 0.02°E), each of which scanned the Chelyabinsk region at ~0327 UTC.

The MSG satellites provided multispectral views including the 3.9-μm near-infrared band from their Spinning Enhanced Visible and Infrared Imager scanning radiometer instruments, which showed what appeared to be a relatively "warm" debris trail; a signature that may be taken as consistent with the fireball observed from the surface. However, harkening back to the discussion about the nature of these scanning radiometer sensors, this hot-target interpretation is not correct. When expressed in terms of an equivalent blackbody (brightness) temperature, the 3.9-μm measurement can appear warm if solar reflection is present. In this case, sunlight reflecting off small particles of the debris trail contributed to the received energy, producing elevated 3.9-μm brightness temperatures (~40 K warmer than the surrounding scene). This apparent warmth is thus a radiometric artifact that should not be misconstrued as sensible heat from the plume. Fig. 1 compares 3.9- and 10.8-μm brightness temperatures from Meteosat-9, revealing much cooler temperatures for the trail at 10.8 μm (which contains no solar component, providing a better metric for assessing the thermodynamic temperature).

Fig. 2 shows two distinct views of the meteor debris trail from DMSP F-16 and Meteosat-9. Fig. 2, *Inset*, shows a surface-based perspective (facing south) of the debris trail. Perhaps the most noteworthy structure along the trail is a convective "turret," corresponding roughly to the level of maximum energy deposition and approximate origination of the sonic blast wave felt in Chelyabinsk. The western side of this turret, shaded from the

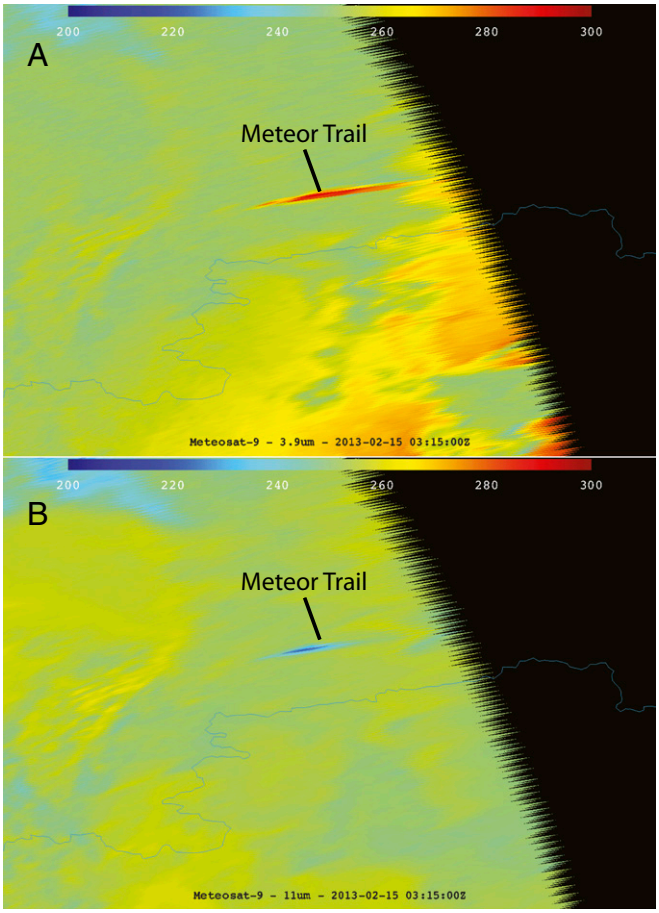

Fig. 1. Meteosat-9 comparison between near-infrared (*A*) and thermal infrared window (*B*) brightness temperatures for the Chelyabinsk meteor trail. Here, "warm" brightness temperatures indicated in the near-infrared imagery can be misinterpreted as a heat signature from the initial meteor fireball. In fact these brightness temperatures are enhanced by contributions from solar reflection and therefore do not represent the thermodynamic temperature of the feature (similarly warm meteorological clouds reside in to the south of the trail). In contrast, the thermal infrared window band reveals the more representative cold thermodynamic temperatures associated with the trail.

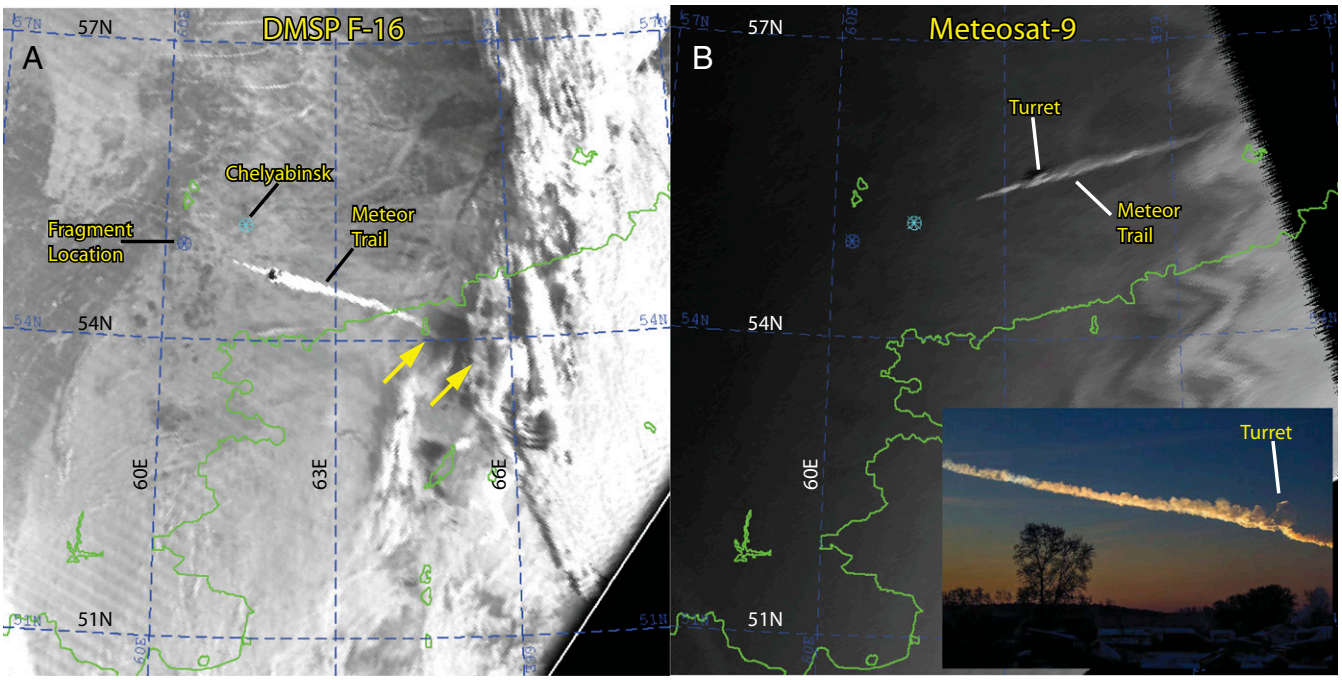

Fig. 2. Comparison of meteor debris trail as viewed (*A*) from the northwest by DMSP F-16 (58.54°N, 45.65°E; 833 km) and (*B*) from the southwest by Meteosat-9 (0.19°N, 9.41°E; 35,786 km). The location of Chelyabinsk and the location of a meteorite fragment that left an ∼6 m hole in a frozen lake near the town of Chebarkul are also shown. Viewing parallax-effect results in dramatic displacement of the trail from its true nadir ground track; the Meteosat-9 imagery suggests a trajectory northeast to southwest trajectory crossing almost directly over Chelyabinsk, whereas the DMSP F-16 imagery suggests a trajectory from southeast to northwest and passing by south of the city. Strong upper-level west/northwesterly winds (>80 m/s; shown in Fig. S7) have begun to shear the originally straight-line meteor trail to the south by the time of the F-16 overpass (yellow arrows in *A*). A surface-based view of the meteor trail, looking toward the south from Chelyabinsk, is shown in the *Inset*. Given the photographer's perspective, the orientation of the trail is approximately reversed from how it appears in the satellite imagery.

morning sun, is clearly evident in both the DMSP F-16 imagery (dark pixels) and surface photography. Thermal infrared (11.0 μm) measurements from DMSP F-16 (Fig. S6) indicate that temperatures at the top of the turret were about −67° C. This places the turret in the middle stratosphere (25–30 km), according to corresponding sounding analysis data from the European Centre for Medium-range Weather Forecasts (ECMWF; Fig. S7), an estimate consistent with the more detailed geometry estimates to follow.

When viewing 2D satellite imagery it is sometimes difficult to appreciate the true 3D structure of the scene. Oblique viewing geometries can provide a better perspective. The unique Earth-limb viewing perspective on the event offered by MTSAT (Fig. 3) clearly illustrates the effects of this strong wind shear on the space/time evolution of debris trail structure. A slight southward curvature to the expected straight-line meteor trail is discernible in the F-16 imagery (see yellow arrows in Fig. 2). According to the matched ECMWF upper-level wind analysis (provided up to 60 km; Fig. S7), light northerly winds between 20 and 30 km gave way to stronger west/northwesterlies at higher levels (80–100 m/s between 50 and 60 km). If this trend continued at higher altitudes, near the beginning of the trail, it could account for noticeable curvature over the ∼5 min of elapsed time until first observation. Researchers have recently demonstrated the utility of such observations for deriving the upper-atmospheric wind profile, based on surface camera views of a persistent meteor trail over Antarctica (9).

Of particular interest in Fig. 2 is the apparent disagreement in azimuthal orientation of the meteor trail when viewed from the different satellites. Meteosat-9, from its southwestern viewing perspective on the Chelyabinsk region, shows the trail oriented in a northeast-to-southwest direction (azimuth angle of $\phi = 253.9°$, defined clockwise from north = 0°). Meanwhile, DMSP F-16, which viewed the region from a west/northwestern perspective and approximate subsatellite location of (58.54°N, 45.65°E), suggests a southeast-to-northwest direction of travel ($\phi = 287.8°$). The apparent displacement of the trail as viewed from the two satellites is significant—to the extent that it almost appears as separate events. In fact, among all satellites viewing the meteor trail, no two were in full consensus on its location or azimuth of trajectory.

The apparent trajectory disagreements are an extreme example of the parallax effect (10–12), where objects viewed from an oblique (nonnadir) perspective are displaced away from the observer radially from their true nadir-equivalent surface locations when map projected to an assumed ellipsoid. The displacement effects are most pronounced for high-altitude objects being viewed at high observer zenith angles. Whereas for most tropospheric clouds and viewing conditions, parallax effects are minor, they become significant for an upper-atmospheric feature observed near the limb of satellite field of regard. Thus, in Fig. 2 the southwestern viewing perspective of Meteosat-9 results in a displacement of the trail to the northeast, and a west/northwestern view of DMSP F-16 displaces it to the east/southeast. The parallax effects are further complicated by the varying altitude of the trail (which descends through the atmosphere along a constant angle), resulting in an elongation of the trail and an alteration of its apparent azimuth of trajectory.

An Estimate of True Trajectory

The unique displacements observed by each satellite can be used to approximate the meteor trail's true location, height, and orientation. The *Methods* section describes the procedure followed in estimating these parameters, based here on the nearly coincident (<2 min) observations of DMSP F-16 and Meteosat-9.

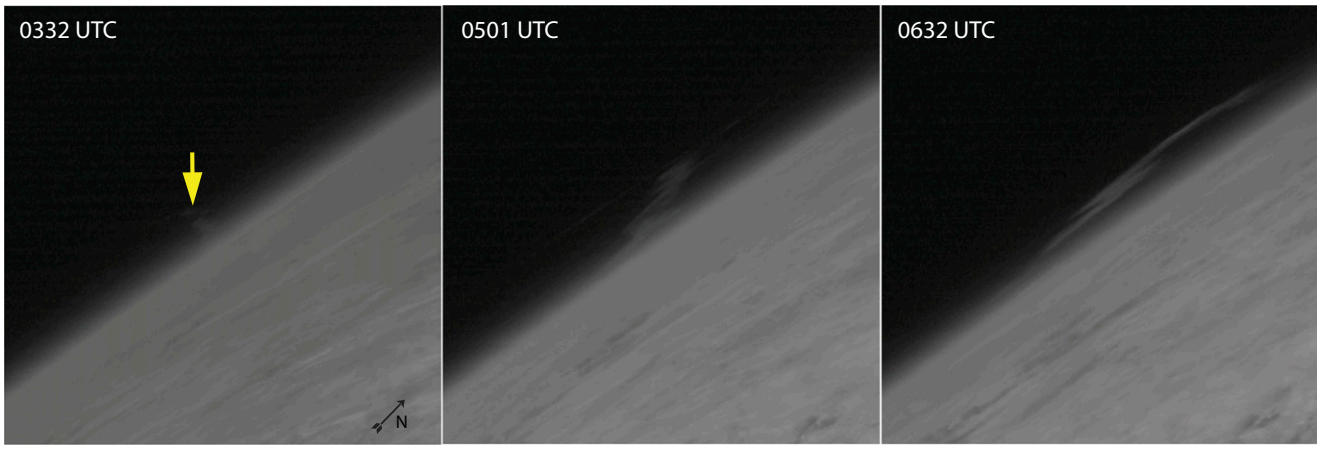

Fig. 3. Evolution of Chelyabinsk meteor trail over a 3-h period (0332–0632 UTC, February 15, 2013) as observed from the MTSAT, a geostationary satellite. From the extreme southeast perspective of this geostationary satellite (situated over the equator at 140°E, viewing the Chelyabinsk region at 55.17°N, 61.40°E) the plume is observed on the Earth's limb. The topmost portions of this plume were estimated to reside near 90 km altitude. Strong speed and directional vertical wind shear in the stratosphere and mesosphere resulted in rapid advection and distortion of the meteor trail from its original straight-line trajectory.

The results of this analysis are shown in Figs. 4 and 5. The derived ground track, whose trajectory azimuth angle of $\phi = \sim 282.7°$ falls in between those suggested by the uncorrected satellite perspectives, is consistent with expected parallax effects for these viewing geometries. Based on the calculated slope to the horizontal (~18.5°) and nadir ground-track distance (~201.1 km), we estimated the satellite-discernible visible plume distance as ~212.1 km. Coupling this information with surface-based video footage, which shows that ~12 s elapsed during formation of the visible trail seen in the satellite imagery, we estimated an average air speed of ~17.7 km/s. The computed ground-track azimuth is consistent with projection to the location of the ~6 m wide hole in the ice of Lake Chebarkul, but requires a steeper angle of entry as opposed to a simple extrapolation of the straight-line path, suggesting a decelerated, parabolic descent of the fragment as it fell through the lower atmosphere.

The greatest sources of uncertainty in the satellite-based estimates are identification of common features between the two satellite perspectives of the debris trail, done here by visual inspection of the imagery, and determining the exact starting point of the tenuous meteor trail. Estimated uncertainties in the turret feature [0.06°, 0.12°, 1.9 km] and end point [0.05°, 0.10°, 0.8 km] translated to corresponding uncertainties of 2.3° in trajectory azimuth angle, 3.8° in incidence angle, and 0.5 km/s in air speed.

The satellite-derived estimates of meteor trajectory and speed were compared against preliminary surface video-based estimates made by the Astronomical Institute of the Academy of Sciences, Ondrejov, Czech Republic. This group identified the

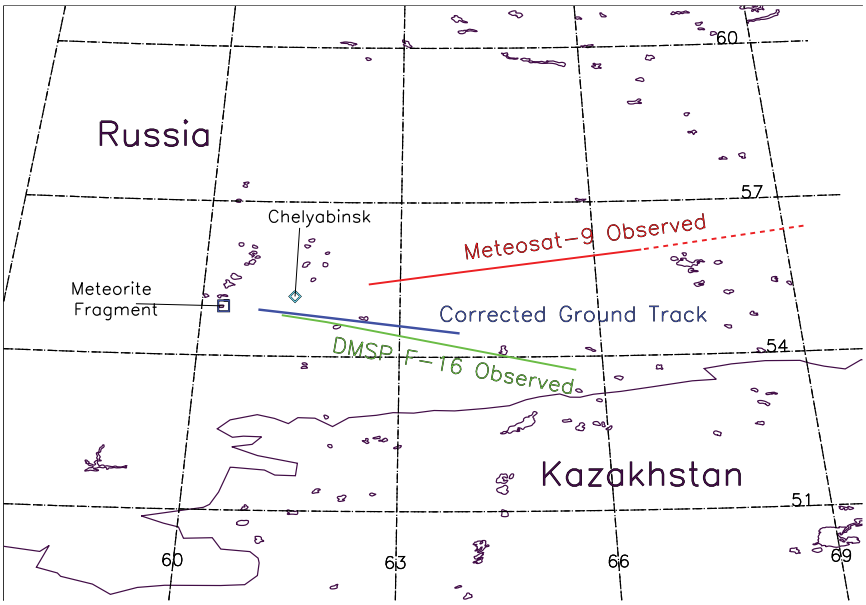

Fig. 4. Comparison between uncorrected (satellite-mapped features as shown in Fig. 2) and corrected (blue) ground tracks for the Chelyabinsk meteor trail. Dashed portion of the Meteosat-9 trajectory (red) was deduced (extending beyond the limb of satellite's field of regard) from the observed F-16 trail extent. Parallax effects displace the apparent position of the trail location away from the satellite-viewing direction, and elongate it due to the increasing height of the trail from west to east. The DMSP F-16 trail (green) is displaced mostly eastward due to the satellite's western perspective, whereas the extreme southwestern perspective and higher viewing zenith angles of Meteosat-9 result in relatively stronger parallax shifting effects.

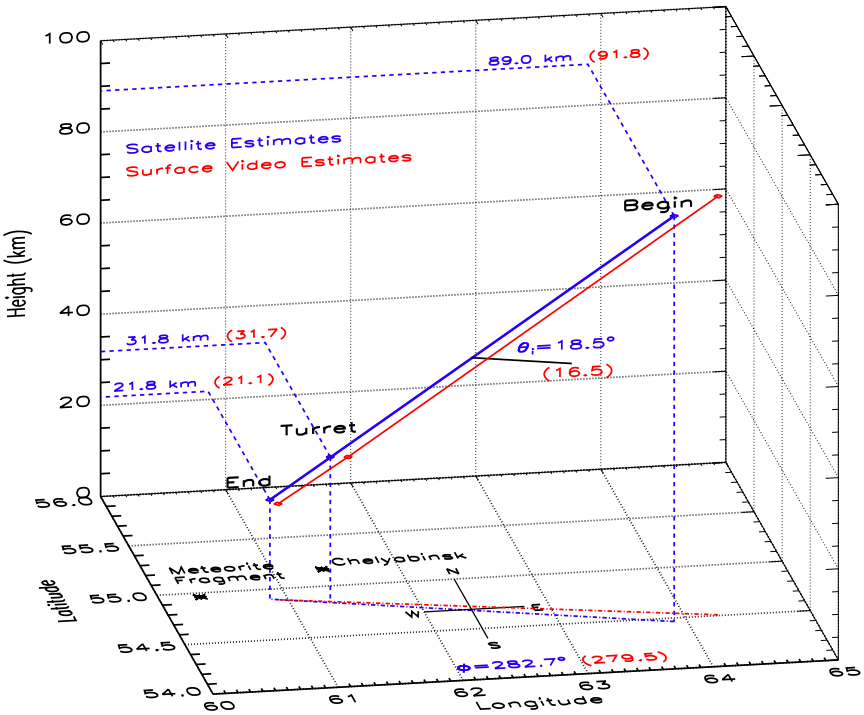

Fig. 5. Satellite-derived (blue) and surface-based video (red) 3D reconstruction of the Chelyabinsk meteor trajectory showing the approximate vertical extent and incident angle (with respect to the horizontal) of the observed meteor trail. For the satellite estimates, the turret feature (Fig. 2) and trail endpoint were used as matching features between Meteosat-9 and DMSP F-16 for these calculations.

locations of seven publicly available casual videos, using Google Maps tools to identify visible landmarks (13). Azimuth and elevation angles of the landmarks as seen from the video location were computed. For comparison against these landmarks, they estimated the azimuth and elevation of the meteor at different phases of its flight in each video. From these data, the meteor trajectory was calculated via the straight least squares method (14).

These video-derived results are included on Fig. 5 in red notations. The Czech group estimates uncertainty of the trajectory positions as 4 and 1 km at the beginning and ends of registration, respectively. The satellite-derived latitude/longitude/altitude coordinates for the begin, turret, and end points (shown in Fig. 5) are (54.5°, 63.9°, 89.0 km), (54.8°, 61.3°, 31.8 km), and (54.9°, 60.9°, 21.8 km), respectively; and the corresponding points for the video-based estimates are (54.51°, 64.27°, 91.83 km), (54.84°, 61.46°, 31.73 km), and (54.89°, 60.92°, 21.05 km). The two independently derived trajectories were found to be in reasonable agreement, particularly when considering the uncertainties associated with common-feature identification in the satellite-based estimates.

Concurrent to this writing, there is a burgeoning cadre of research surrounding the Chelyabinsk superbolide. This includes other video-based orbit reconstructions (1), meteoroid ablation process estimates (15), and other reconstructions of trajectory and orbital parameters based on alternative sets of satellite observations to what has been considered here (16). Analysis of these various findings is an ongoing process, subject to revision and improvement, with each study contributing a new data point to the growing scientific record. In this spirit, a campaign dedicated to gathering all manner of further technical information about the Chelyabinsk event is ongoing at www.russianmeteor2013.org. These activities will help to cultivate already fertile soil for collaborative research concerning this extraordinary astronomical event.

Conclusions and the Positive Impacts of Future Sensors

A combination of geostationary and low-Earth-orbiting meteorological satellites captured a unique perspective on the Chelyabinsk superbolide within several minutes of debris trail formation. Ostensibly, these observations painted an inconsistent picture of the object's trajectory, due to extremely strong parallax displacement effects incurred from oblique viewing of the high-altitude debris trail. Given the geometry of the satellites at the time of their observations, the displacements were used to back out the true trajectory. The estimates compared favorably to independently derived surface-based camera/video estimates. In so doing, these Earth-viewing environmental satellites have demonstrated their value as a useful, albeit unconventional, tool in trajectory reconstructions.

The international community of environmental satellite data providers will be upgrading their geostationary observing capabilities substantially over the coming decade. For example, Geostationary Operational Environmental Satellite (GOES-R), the next generation US geostationary series, which is slated to launch in late 2015, will offer two Earth-facing instruments bearing relevance to meteor detections. The Advanced Baseline Imager (17) will provide improved spatial, spectral, temporal, and radiometric resolution compared with current-generation sensors. GOES-R will also carry the Geostationary Lightning Mapper (18), a staring optical instrument that could detect transient visible light emissions associated with a meteor if it passed within the sensor's field of regard. Europe and other geostationary satellite providers will be making similar upgrades to their next-generation sensor suites. The same measurements and trajectory-estimation techniques demonstrated here would also apply in a more general sense to atmospheric condensation trails produced by terrestrial sources, such as aircraft and rockets.

In the wake of the Chelyabinsk event, more attention is being paid to preemptive measures as well, particularly in the context of larger bodies such as asteroids. The European Space Agency announced a new joint satellite mission study with the United

States: the Asteroid Impact & Deflection Assessment. This mission would target an asteroid and measure orbital changes resulting from a prescribed impact. Privately funded missions such as the B612 Sentinel, propose similar kinetic impactors means to deflecting an asteroid's trajectory, with detection lead time playing a key role in efficacy. In terms of detection and tracking of potential hazards, there exist long-established programs including the Massachusetts Institute of Technology Lincoln Near Earth Asteroid Research (LINEAR) program, the National Aeronautics and Space Administration Near Earth Object Program, and the Meteoritical Society (http://meteoriticalsociety.org). Based on these sources, it is estimated that there are roughly 1,000–2,000 bodies with diameter >1 km in near-Earth orbits (approach within 1.3 AU of the Sun), equating to a ∼1% chance of collision with Earth in the next millennium (19).

In fact, just hours after the Chelyabinsk event, a much larger object (2012 DA_{14}, ∼45 m diameter) passed below the geostationary orbits to within 27,000 km of Earth—a very close call by astronomical standards. The object was of a size class on par with the 1908 Tunguska event as well as the Canyon Diablo meteorite (∼50 m, 300–400 kilotons, and 20–40 megatons of impact kinetic energy), which produced the Barringer Crater in northern Arizona 49,000 ya (20, 21). The Chelyabinsk meteoroid, based on petrographic studies from recovered fragments of its mineral composition (ordinary chondrite; ref. 22), is estimated to have derived from the main asteroid belt (22), and is thought to be unrelated to the 2012 DA_{14} asteroid.

The question of possible relationship between the nearly concurrent arrivals of the February 2013 objects was a natural one to ask, however, and underscores a point of immediate practical relevance to this study. In the event of a remote (i.e., far removed from a gallery of Russian dash cams) event, the global constellation of Earth-viewing satellites is far more likely to be in a position to assess trajectory and infer the source. If used in synergy with other warning and decision aid systems, including resources designed for this purpose, these satellites could play a complementary role in more rapidly directing our attention and response with regard to possible follow-up threats (e.g., in the case of binary or triple asteroid systems, which are thought to account for ∼15% of the near-Earth asteroid population, ref. 23).

Methods

Multiview geometric-based methods have proven useful for meteor trajectory estimation (24). Details of the satellite-derived meteor trail geometry were determined from joint observations by DMSP F-16 and Meteosat-9, which observed the region at 0324:40 and 0326:26 UTC, respectively. Feature displacements over the time differences between the two satellite views and the meteor entry (0320:30 UTC) were assumed small. Features common to the two satellite images (end of the trail and a convective turret) were used as reference points for the calculations. Beginning at the apparent (parallax-affected) feature-pair locations, the feature's height (H) was increased iteratively. A ground distance [$d = H \tan(\theta_s)$; where θ_s = satellite zenith angle] was traversed in an azimuthal direction leading back toward each satellite's subpoint. The difference between the end points of these two traverses was calculated, and the H minimizing this difference yielded the estimated feature height. The mean value of the traverse end points (latitude and longitude) corresponding to the retrieved H was used as the best-estimate nadir-surface location of that feature. Repeating this procedure for two distinct features along the plume provided sufficient information to estimate several additional parameters, including: azimuth and vertical incidence angles, trail length, height at point of initial formation, and with the assistance of surface video, and air speed.

ACKNOWLEDGMENTS. The efforts of our reviewers in improving this manuscript are gratefully acknowledged. Jiri Borovicka (Astronomical Institute of the Academy of Sciences), Stefan Geens (Ogle Earth), and Sebastian Pauleau (GroupeBolide) provided information on surface-based video meteor trajectory derivations. Jorge Zuluaga (University of Antioquia), Josep Trigo-Rodríguez (Institute for Space Studies of Catalonia), Simon Proud (University of Copenhagen) and Jia Yue (Hampton University) provided further insightful discussions and references. Jeffery Cox (Aerospace Corporation) assisted with a DMSP sensor data inquiry, and Pamela Schoebel-Pattiselanno (EUMETSAT) assisted with Meteosat data requests. S.D.M. acknowledges support from the Naval Research Laboratory (Contract #N00173-10-C2003), the Oceanographer of the Navy through office at the Program Executive Office C4I & Space/Program Manager, Warfare-120 under program element PE-0603207N.

1. Ivanova, MA, et al. (2013) Fall, searching and first study of the Chelyabinsk meteorite. *Abstracts of the 76th Annual Meeting of the Meteoritical Society* 48(s1):5366.
2. Ceplecha Z, et al. (1999) *Meteoroids 1998*, eds Baggaley WJ, Porubcan V (Astronomical Institute Slovak Academy of Science, Bratislava), pp 37–54.
3. Kring DA, Swindle TD, Zolensky ME (2013) Brecciated Chelyabinsk near-Earth asteroid and its catastrophic air burst. *Abstracts of the 76th Annual Meeting of the Meteoritical Society* 48(s1):5224.
4. Brown P, Spalding RE, ReVelle DO, Tagliaferri E, Worden SP (2002) The flux of small near-Earth objects colliding with the Earth. *Nature* 420(6913):294–296.
5. Chyba C, Thomas P, Zahnle K (1993) The 1908 Tunguska explosion: Atmospheric disruption of a stony asteroid. *Nature* 361(6407):40–44.
6. Kidder SQ, Vonder Haar TH (1995) *Satellite Meteorology: An Introduction* (Academic Press, San Diego).
7. Stephens GL, et al. (2002) The CloudSat Mission and the A-Train: A new dimension of space-based observations of clouds and precipitation. *Bull Am Meteorol Soc* 83:1771–1790.
8. Winker DM, et al. (2010) The CALIPSO mission: A global 3D view of aerosols and clouds. *Bull Am Meteorol Soc* 91:1211–1229.
9. Suzuki H, et al. (2013) Inertia-gravity wave in the polar mesopause inferred from successive images of a meteor train. *J Geophys Res* 118D(8):3047–3052.
10. Hasler AF (1981) Stereographic observations from geosynchronous satellites: An important new tool for the atmospheric sciences. *Bull Am Meteorol Soc* 62:194–212.
11. Shenk WE, Curran RJ (1973) A multi-spectral method for estimating cirrus cloud top heights. *J Appl Meteorol* 12:1213–1216.
12. Simpson JJ, McIntire T, Jin Z, Stitt JR (2000) Improved cloud top height retrieval under arbitrary viewing and illumination conditions using AVHRR data. *Remote Sens Environ* 72:95–110.
13. Borovicka J, Spurny P, Shrbeny L (2013) Trajectory and orbit of the Chelyabinsk superbolide [Electronic telegram]. Electronic telegram 3423 (Central Bureau for Astronomical Telegrams, International Astronomical Union, Cambridge, MA).
14. Borovicka J (1990) The comparison of two methods of determining meteor trajectories from photographs. *Bull Astron Inst Czech* 41:391–396.
15. Dergham J, Trigo-Rodríguez JM (2013) The dynamical behaviour of the Chelyabinsk superbolide by using a Runge-Kutta algorithm. European Planetary Science Congress 2013 London, id. EPSC2013-1003.
16. Proud S (2013) Reconstructing the orbit of the Chelyabinsk meteor using satellite observations. *Geophys Res Lett* 10.1002/grl.50660.
17. Schmit TJ, et al. (2005) Introducing the next-generation advanced baseline imager on GOES-R. *Bull Am Meteorol Soc* 86:1079–1096.
18. Goodman SJ, et al. (2013) The GOES-R Geostationary Lightning Mapper (GLM). *Atmos Res* 125-126:34–49.
19. Rabinowitz D, Helin E, Lawrence K, Pravdo S (2000) A reduced estimate of the number of kilometre-sized near-Earth asteroids. *Nature* 403(6766):165–166.
20. Artemieva N, Pierazzo E (2009) The Canyon Diablo impact event: Projectile motion through the atmosphere. *Meteorit Planet Sci* 44:25–42.
21. Artemieva N, Pierazzo E (2011) The Canyon Diablo impact event: 2. Projectile fate and target melting upon impact. *Meteorit Planet Sci* 46:805–829.
22. Liu Y, et al. (2013) Chelyabinsk: An ordinary chondrite from a spectacular fall in Russia. *Abstracts of the 76th Annual Meeting of the Meteoritical Society* 48(s1): 5103.
23. Walsh KJ, Richardson DC, Michel P (2008) Rotational breakup as the origin of small binary asteroids. *Nature* 454(7201):188–191.
24. Jones J, et al. (2005) The Canadian meteor orbit radar: System overview and preliminary results. *Planet Space Sci* 53:413–421.

Supporting Information

Miller et al. 10.1073/pnas.1307965110

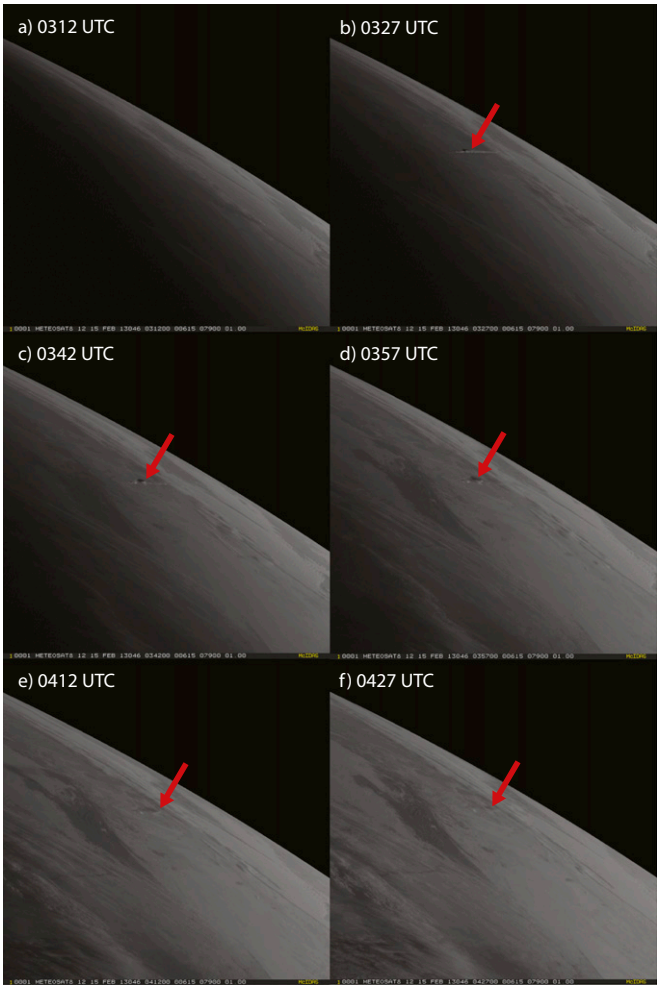

Fig. S1. Meteosat-8 (4.2°E) sequence of visible-band imagery showing the Chelyabinsk meteor trail formation and its evolution at 15-min intervals. The first image of the sequence (*A*) was collected before impact, and the remaining images of the sequence (*B*–*F*) show the formation and drift of the trail. These data have been remapped to a 9.5° E reference location, providing additional eastern coverage.

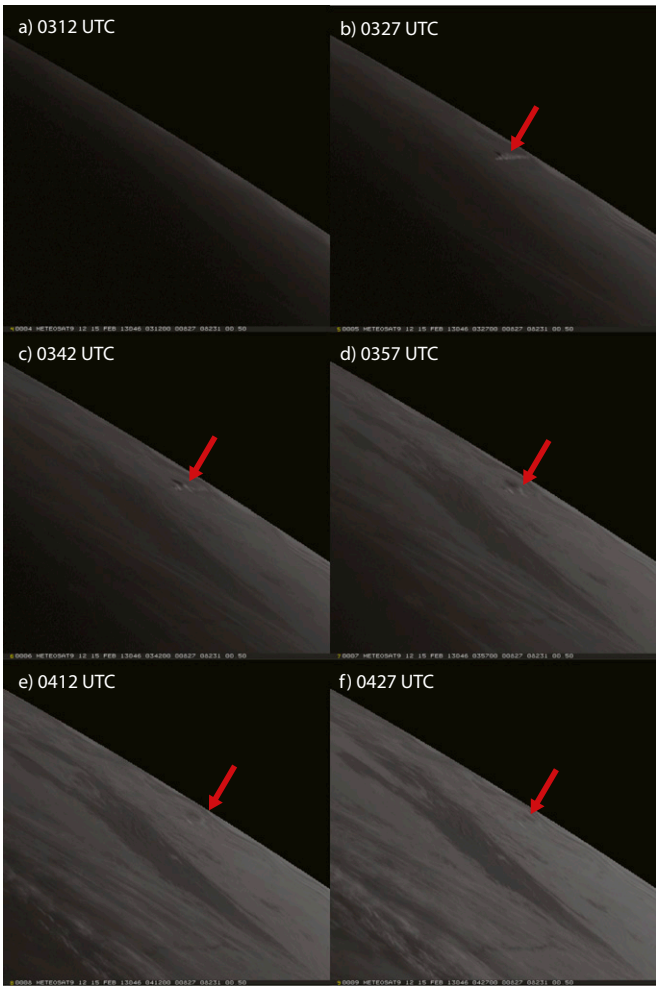

Fig. S2. As in Fig. S1, but as viewed from Meteosat-9 (9.5°E), showing imagery just prior to impact (*A*) and subsequent imagery (*B*–*F*) showing formation and drift of the meteor trail. Unlike the Meteosat-8 imagery, this image was remapped to a 0° longitude reference location. This explains why the edge of imagery coverage is slightly west of Meteosat-8, despite Meteosat-9's subpoint being 5° farther to the east.

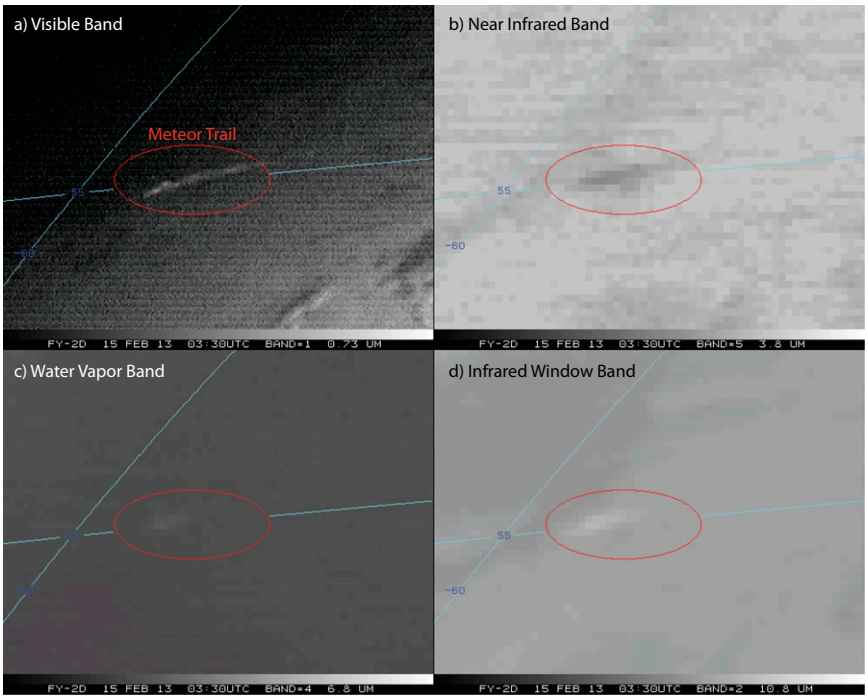

Fig. S3. Feng-Yun 2D (86.5°E) multispectral imagery of the Chelyabinsk meteor trail 0330 UTC collection time (0332 UTC actual scan time, or roughly 12 min after trail formation). The visible (0.73 μm), near-infrared (3.8 μm), "water vapor" (6.8 μm), and far-infrared (11.0 μm) bands are shown in (*A*–*D*), respectively. The signature of the meteor trail is present in each of the bands. For the infrared bands, a darker color corresponds to a warmer brightness temperature.

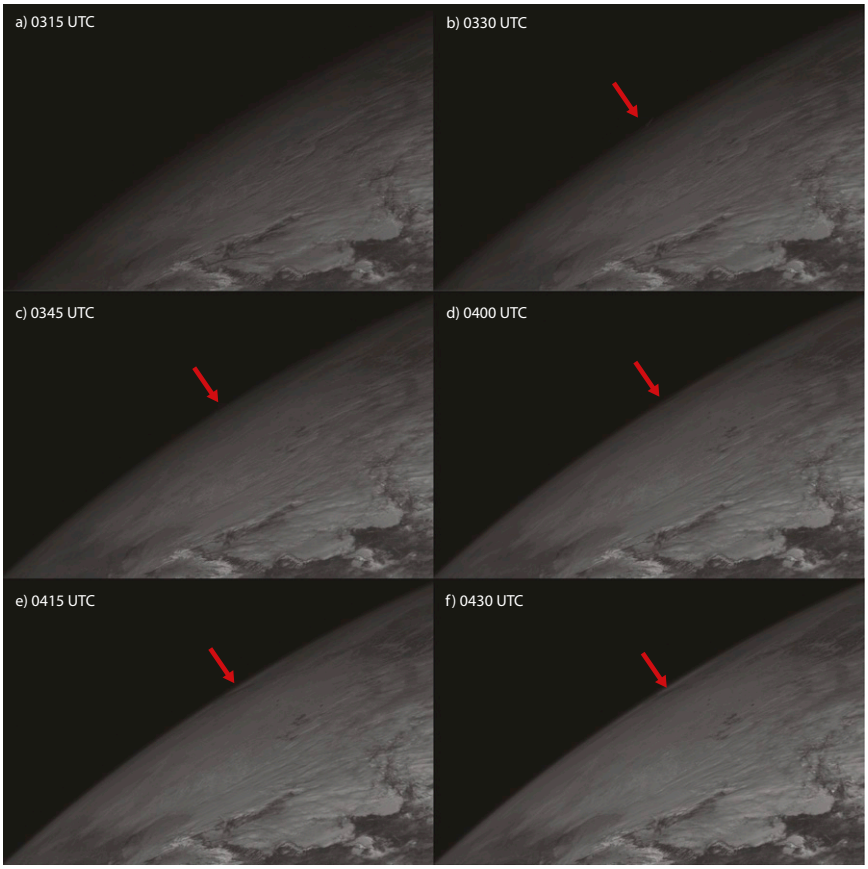

Fig. S4. As in Fig. S1, but as viewed from the Communication, Ocean, and Meteorological Satellite (COMS; Korean Meteorological Administration), showing imagery just prior to impact (*A*) and subsequent imagery (*B*–*F*) of formation and drift of the meteor trail. From this satellite's vantage point at 128.2°E, the meteor trail nearly blends in completely with the limb of the earth.

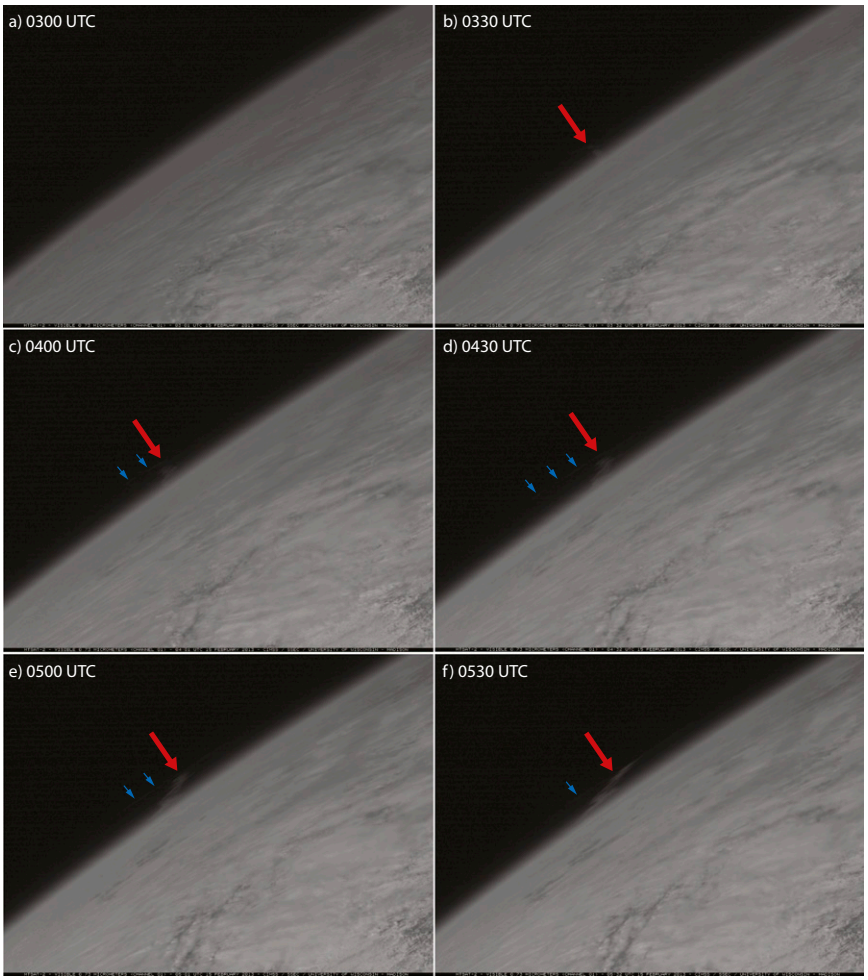

Fig. S5. As in Fig. S1, but as viewed from Multifunctional Transport Satellite (140°E), showing imagery from just before impact (*A*) and subsequent imagery (*B*–*F*) showing formation and drift of the meteor trail. From this satellite's unique vantage point, the trail is observed well above the Earth's limb and provides good contrast against the darkness of space. Blue arrows denote faint portions of the initial meteor trail which were being advected rapidly to the east/southeast by strong upper-level winds.

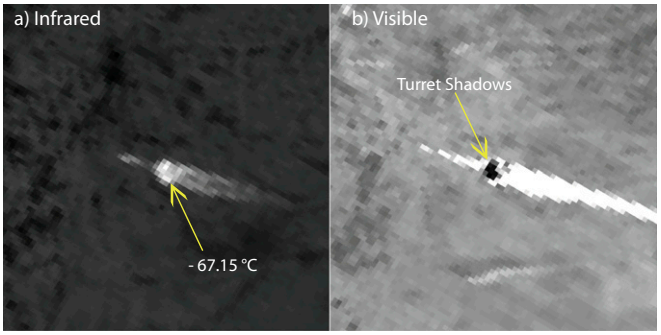

Fig. S6. Defense Meteorological Satellite Program (DMSP) constellation F-16 satellite and its Operational Linescan System (OLS) sensor (*A*) infrared (11.0 μm) and corresponding (*B*) visible (0.6 μm) imagery zoomed in on the Chelyabinsk meteor trail, collected on 15 February 2013 at 0324:40 UTC. The scale of this scene is 200 km on a side. The −67.15 °C infrared brightness temperature of the optically thick "turret" feature (*Fig. 2*, *Inset*) places this feature in the lower stratosphere, consistent with geometric calculations.

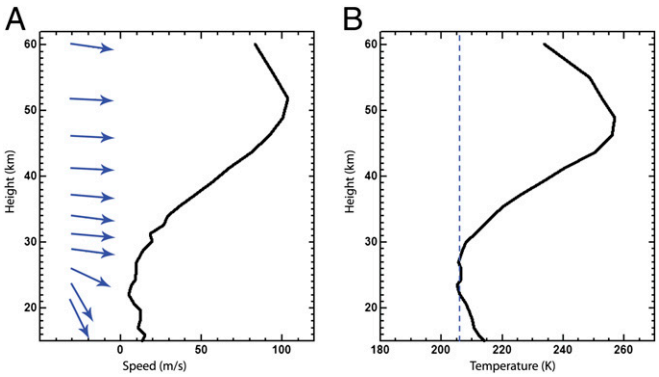

Fig. S7. Profiles of (*A*) wind direction (arrows; up = north, right = east) and speed, and (*B*) temperature between 15 and 60 km from European Centre for Medium-range Weather Forecast model fields, valid on 15 February 2013 at 0300 UTC for the closest model grid point (0.5° grid resolution; 55°N, 61°E) to the Chelyabinsk meteor event. The dashed blue line on the temperature plot corresponds to the DMSP F-16 OLS-measured turret temperature of −67.15 °C (= 206 K; Fig. S6).